BIODIVERSITAS
Volume 24, Number 9, September 2023
Pages: 5022-5034

ISSN: 1412-033X
E-ISSN: 2085-4722
DOI: 10.13057/biodiv/d240946

Morphological and anatomical studies of *Conamomum vietnamense* N.S. Lý & T.S. Hoang: An endemic plant from Vietnam

NGUYEN THANH TO NHI[1], TRAN VAN CHEN[2,♥], DUONG NGUYEN XUAN LAM[3], DANH DUC NGUYEN[4], QUANG DIEP DINH[5], NGUYEN HOANG KHANH LINH[1]

[1]Faculty of Pharmacy, Nguyen Tat Thanh University, Ho Chi Minh City. No. 300A, Nguyen Tat Thanh Street, Ward 13, District 4, Ho Chi Minh City 70000, Vietnam
[2]Faculty of Traditional Medicine, University of Medicine and Pharmacy at Ho Chi Minh City. No.217, Hong Bang Street, Ward 11, District 5, Ho Chi Minh City 70000, Vietnam. Tel./fax.:+84-866-486674, ♥email: tvchenpharma@ump.edu.vn; tvchenpharma@gmail.com
[3]Faculty of Pharmacy, University of Medicine and Pharmacy at Ho Chi Minh City. No. 217, Hong Bang Street, Ward 11, District 5, Ho Chi Minh City 70000, Vietnam
[4]Institute of Applied Technology, Thu Dau Mot University. No. 06, Tran Van On Street, Phu Hoa Ward, Thu Dau Mot City 7510, Binh Duong Province, Vietnam
[5]Nong Lam University. Quarter 6, Linh Trung Ward, Thu Duc City, Ho Chi Minh City 70000, Vietnam

Manuscript received: 20 July 2023. Revision accepted: 27 September 2023.

Abstract. *Nhi NTT, Chen TV, Lam DNX, Nguyen DD, Dinh QD, Linh NHK. 2023. Morphological and anatomical studies of* Conamomum vietnamense *N.S. Lý & T.S. Hoang: An endemic plant from Vietnam. Biodiversitas 24: 5022-5034. Conamomum vietnamense* N.S. Lý & T.S. Hoang (Zingiberaceae) is an endemic plant from Vietnam. Information on the anatomical structure of leaves, roots, rhizomes, and the powder characteristics of *C. vietnamense* has not been reported. This study aimed to combine macro- and micro-morphological analysis to identify *C. vietnamense* accurately. Twenty fresh plants were randomly collected from the wild habitats in Vietnam were used for the study. Macromorphological characteristics were observed and compared to earlier research. Iodine green-carmine staining was then used to histologically examine the leaves, roots, and rhizomes. The powdered rhizome and leaf features were described via a microscope. Macromorphologically, *C. vietnamense* is characterized by its stout stilt roots, short petioles, oblong-lanceolate leaf blades with lightly plicate, inflorescences with obovoid, and narrowly ovate bracts, hairy underside bracteoles, bilobed calyx, yellow flowers with broadly obovate, glabrous, trilobed labellum. Micromorphologically, the anatomical features of leaves, roots, and rhizomes have similarities with those of Zingiberaceae species. The tetracytic stomata was observed on both leaf surfaces. The stomatal indexes on the abaxial and adaxial surfaces of the leaves are 8.81±0.55% and 0.1±0.06%, respectively. Calcium oxalate crystals were found in the leaf. Starch grains and reticulate xylem vessels were present only in rhizome powder. These findings are important characteristics for identifying *C. vietnamense*.

Keywords: Anatomical structure, *Conamomum vietnamense*, endemic plant, macromorphological, micromorphological, powder

Abbreviations: ddw: double distilled water; SI: Stomatal Index

INTRODUCTION

Conamomum Ridl. is a small genus of the ginger family (Zingiberaceae) first reported by Ridley (1899). The genus was assigned to the genus *Amomum* Roxb. by Holttum (1950). In other words, it is considered a synonym of the genus *Amomum* (Lamxay and Newman 2012). Boer et al. (2018) resurrected the genus *Conamomum* based on morphological features and molecular (nrITS and *matK*) evidences. Thus, globally, there are currently about 12 accepted species in the genus *Conamomum* (POWO 2023), which is distributed mainly in the wet tropical biome, i.e., primary evergreen lowland and montane forests from the Indochinese region (Vietnam, Cambodia, and Thailand) to the West Malesia region (Malaysia, Singapore, Borneo, and Sumatra) (Ly et al. 2022). During the field investigation on the diversity of essential oil plants in Vietnam, four species, namely *Conamomum rubidum* (Lamxay & N.S. Lý) Škorničk. & A.D. Poulsen, *C. odorum* Luu, H.Đ. Trần & G. Tran, *C. pierreanum* (Gagnep.) Škorničk. & A.D. Poulsen, and *C. vietnamense* N.S. Lý & T.S. Hoang) of were reported in Vietnam (Truong et al. 2019; Luu et al. 2021; Ly et al. 2022; POWO 2023). The genus *Conamomum* has always posed challenges for classification based on morphological features because detailed morphological studies show that *C. vietnamense*, an endemic species from Vietnam, is reported to be most similar to *C. odorum* and *C. rubidum* (Ly et al. 2022).

A previous study reported that the essential oils of the rhizomes and leaves of *C. vietnamense* are effective against pathogenic microorganisms (Nguyen et al. 2023). However, except for the essential oil and its anti-bacterial activity, the other information about *C. vietnamense* has not yet been investigated further. The high degree of morphological complexity and diversity has made identifying *C. vietnamense* more difficult when relying on traditional morphological methods. Accurate species identification is important for correctly searching and using medicinal plants. There are many causes for the external morphological variation or diversity between species in the genus, such as

polyploidization and hybridization, distinctive levels of genetic and morphological variation, as well as the similarity macro-morphological. All of which contributed to the difficulty of identifying them (Anu et al. 2020; Van Chen et al. 2022a, 2022b; Windarsih et al. 2021; Ly et al. 2022).

Macro-morphological characters of *C. vietnamense* has been described in detail by Ly et al. (2022), however, detailed descriptions of its micro-morphological characteristics have not yet been published. Therefore, the identification of micro-morphological characteristics of *C. vietnamense* becomes extremely necessary. Traditionally, macro-morphological characteristic description is the traditional method for taxonomy; but with the assistance of micro-morphological characteristics, plant identification is much more precisely achievable (Alamgir 2017; Van Chen et al. 2022b). By studying the anatomical features of plants, such as rhizomes, roots, leaves, etc., taxonomists can authenticate plant specimens and detect any adulteration or contamination. However, macro-morphological characteristic studies have limited use in authenticating ground or processed spices and herbs. The method of using microscopy to detect impurities in ground spices or herbs is considered useful in identifying raw powder samples (Alamgir 2017; Osman et al. 2019).

Therefore, to provide more scientific information on the botanical characteristics, this study was carried out to combine macro-and micro-morphological analysis to identify *C. vietnamense* from Vietnam accurately. The results obtained in this study would establish the criteria for a monograph to identify *C. vietnamense*; from that, people could choose the correct species and use them as safe medicinal herbs.

MATERIALS AND METHODS

Plant material

Twenty fresh plants were randomly collected from the wild habitat in Loc Bac Commune, Bao Lam District, Lam Dong Province, Vietnam (11°47'31.9" N, 107°35'47.2" E, collector's number: NDD-296). The samples were washed for macro- and micro-morphological analyses. Some leaves and rhizomes were air-dried and powdered to evaluate the powder's characteristics. Two herbarium sheets were repaired and deposited at the Hanoi University of Science Herbarium (HNU), Hanoi, Vietnam.

Procedures

Macro-morphological characteristics

The morphological comparison method was used to determine the scientific name of *C. vietnamense* according to the Vietnamese Pharmacopoeia V standard protocol (Ministry of Health 2017). Regarding surveying macro-morphological characteristics, it is necessary to survey many samples for each plant in the same distribution area (describe and measure the size with a ruler). Hand-held magnifiers are also used to observe the macro-morphological features of the underground parts (stilt roots, rhizomes) and the above-ground parts (leafy shoots, pseudostems, petioles, leaf blades, inflorescences, flowers, and fruits). Then, photograph these parts with a Canon digital camera. Moreover, the samples were compared with the taxonomic key and description prepared by Ly et al. (2022) to identify the species name.

Micro-morphological characteristics

The micro-morphological characteristics were identified using the iodine green-carmine double staining method (Ministry of Health 2017). The steps are as follows: (i) The chopped representative specimens (roots, rhizomes, and leaves) were cut into thin slices (10-20 μm) with a razor blade, (ii) Thin-complete slice sections were used for staining. These samples were cleaned with 5.0% (w/v) chloramine-T and 50% (v/v) chloral hydrate reagents (for 10 min), respectively. They were then acidified in 1.0% (w/v) acetic acid for 2 minutes. Next, 0.3% (w/v) Iodine Green (soak for about 5 seconds only) and 1.0% (w/v) Carmine reagents (until the slices had a clearer color) were used for subsequent dyeing. Double-distilled water (ddw) was used to remove excess reagents (chloramine-T, chloral hydrate, acetic acid, iodine green, and carmine) through the abovementioned steps, (iii) The samples were stored in a glycerin water mixture (1:1), (4) the prepared samples were covered with a coverslip in mixed glycerin water and then observed under a light microscope (HumaScope, Germany) at 4X, 10X, and 40X magnifications (fitted with the ocular micrometer scale). Similarly, leaf powder and rhizome powder characteristics were also observed under the microscope with 10X and 40X magnification (HumaScope, Germany) (Ministry of Health 2017).

The features of the leaf epidermal surface and the stomata were observed under a 40X magnification microscope (Labomed, USA) (WHO 2011; Zahara 2020; Van Chen et al. 2022b). The stomatal index (SI) was also performed (with 20 replicates) to observe the stomatal distribution in both leaf epidermal surfaces. The stomatal index was determined by the following formula described by WHO (2011), Ministry of Health (2017), and Zhao et al. (2022) as follows:

Determination of stomatal index (at 40X magnification):

$$SI\ (\%) = (S/(S+E)) \times 100$$

Where: S and E are the numbers of stomatal and epidermal cells (including trichomes) in the field of view by the microscopy at 40X magnification, respectively (Zahara 2020; Van Chen et al. 2022b).

Data analysis

Macro- and micro-morphologically, the size of the sample parts and cell components were measured using a standard ruler and eyepiece micrometer scale (Olympus, Japan), respectively. Moreover, the stomatal number was counted with 20 replicates; the stomatal index (SI) was determined from that result. All results were analyzed and expressed as mean values ± S.D (Standard Deviation) using Microsoft Excel 2023 (WHO 2011; Van Chen et al. 2022b; Zhao et al. 2022).

RESULTS AND DISCUSSION

Macro-morphological features

Description

Conamomum vietnamense is an herb composed of underground parts (stilt roots, rhizomes) and above-ground parts (leafy shoots, pseudostems, petioles, leaf blades, inflorescences, flowers, and fruits). It is a small clump-forming herb up to 1.5 m tall, with 5-10 pseudostems per clump (Figure 1A). *Rhizome* creeping outside pale green turning brown with age, inside cream white internally, slightly aromatic; rhizome scales broadly triangular, brown, soon decaying; well-developed, stout stilt roots, brown-greenish when young turning dark brown with age (Figure 1D). *Leaves*: mature leafy shoots ca. 1.0 m long, with 9-12 leaves; bladeless sheaths 3-5, 5-30 cm long, glabrous outside, pale green throughout; leaf sheath dark green, striated, glabrous; ligules entire, ca. 5 mm long, leathery, yellowish-green glabrous, margin entire; petiole reduced, leaf blades oblong-lanceolate, lightly plicate, 30-40 x 5-6 cm, leathery, adaxially dark green, glabrous, abaxially light green, glabrous, base attenuate, apex caudate (Figure 1C). *Inflorescences* erect from the base of the youth rhizome, 1-flowered per cincinnati; peduncle 7-10 cm long covered by 5-10 brown, triangular scales, pale green, glabrous; spike oblong-obovoid, 3-5 cm long, 5-7 cm in diam; fertile bracts 30-45 mm, brown, lanceolate; bracteoles tubular with a unilateral split half the length, hairy outside, 20-25 mm long, semi-translucent, reddish brown, minute pubescent outside, apex acute, margin entire and ciliate (Figure 1B). *Flowers* 5-6 cm long; calyx tubular, ca. 1.0 cm, glabrous, reddish, semi-translucent; floral tube 17-20 mm long, reddish and glabrous; dorsal corolla lobe obovate to elliptic, reddish, translucent, shiny, glabrous in both surfaces, dorsal one ca. 30 × 17 mm, lateral ones narrower 28, ca. 28 × 13 mm; labellum broadly ovate, glabrous, trilobed, 35-40 mm long, ca. 30-35 mm wide when stretched, base half tinged red stripes at lateral sides; lateral staminodes minute, 3-5 mm long, red at base, yellow at apex (Figures 1B and 1E). Stamen 25 mm, pale yellow throughout; filament 15 mm long, puberulent throughout; anther ca.10 × 5 mm long, anther crest distinctly 3-lobe (Figure 1F). Epigynous 2, 2-3 mm long, cream yellow, glabrous (Figures 1E and 1F). The ovary is globose to elliptic, ca. 3 × 3 mm, reddish, pubescent, 3-locular (Figure 1G). *Fruit* capsular, smooth, globose, 1.7-1.9 × 1.5-1.7 cm, glabrous. Flowering in April and predicted to extend to Fall.

Distribution and habitat

Conamomum vietnamense is found in the Plateau of Vietnam. It usually grows under the canopy of broadleaf evergreen mixed tropical forests, on well-drained moist soils or hillsides at 600-800 m elevations. The forest habitat of this species is threatened by logging and disturbance for agriculture.

Conservation status

Conamomum vietnamense is assessed as Endangered with EN B2ab, because its area of occupancy (AOO) is less than 500 km^2, it is severely fragmented or occurs at only one location, and it has a continuing decline in its habitat quality (Le Breton et al. 2019). This assessment was based on a scientific publication by Ly et al. (2022), who described and named the species in 2022. Therefore, it is assessed as Endangered (EN B2ab) and should be conserved (Ly et al. 2022).

Taxonomical notes

The macro-morphological characters of *C. vietnamense* collected in Lam Dong province were similar to those described by Ly et al. (2022). However, this species could be distinguished from other species by the features and shapes of the roots, flowers, and leaves as well as by the *Conamomum* taxonomic key of Truong et al. (2019), Luu et al. (2021), and Ly et al. (2022). The *C. vietnamense* stilt roots (>20 cm, above ground) were longer than other species (i.e., *C. pierreanum* (<20 cm), *C. rubidum* and *C. odorum* (with stilt roots absent).

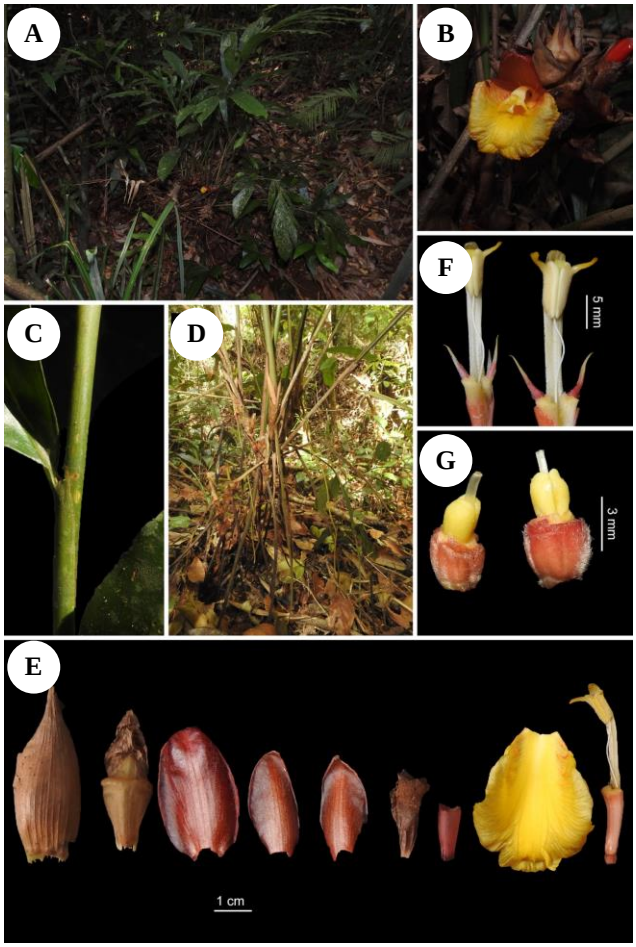

Figure 1. Morphological features of *C. vietnamense*. A. Habitus. B. Inflorescence and flower. C. Leaf and petiole. D. Stilt root and rhizome. E. Bracts, dorsal and lateral corolla lobes, bracteole, calyx tubular, labellum, floral tube and stamen (from left: side view). F. Stamen, filament, anther, and epigynous (front view). G. Ovary and epigynous glands

The petioles of *C. vietnamense* tend to be reduced (about 5-8 mm long), while the ones of *C. pierreanum*, *C. odorum*, and *C. rubidum* are about 20-30 mm, 2-4 mm, and 5-9 mm, respectively. The leaf blade of *C. vietnamense* is oblong-lanceolate and lightly plicate, while the other species are oblong and smooth, except for *C. odorum*, which is narrowly elliptical. The inflorescences of *C. vietnamense* are erect, obovoid, arising from the base of youth rhizomes, compared with *C. pierreanum* (globose to ovoid, erect near the rhizome), *C. rubidum* (obovoid, arising from the base), and *C. odorum* (ovoid, arising from creeping rhizomes). Moreover, the characteristic of the labellum is also a feature that distinguishes these species. Specifically, the labellum shapes of *C. vietnamense*, *C. pierreanum*, *C. odorum*, and *C. rubidum* are obovate-orbicular (broadly ovate), bowl-shaped, obovate, and reniform (kidney-shaped), respectively. In addition, the bilobed calyx, tridentate calyx, pubescent calyx, and glabrous calyx are the distinguishing features of *C. vietnamense*, *C. pierreanum*, *C. odorum*, and *C. rubidum*, respectively (Truong et al. 2019, Luu et al. 2021, Ly et al. 2022). Generally, morphological recognition is perhaps the traditional method used for plant identification, and to some extent, it is still considered efficient and accurate.

Micro-morphological features

Leaves

The leaf cross-section consists of midrib and leaf blades with a symmetrical structure. The upper and lower surfaces of the midrib are slightly concave and parabolic convex, respectively (Figures 2A and 2E). The upper and lower epidermises comprise a single layer with polygonal cells and cellulose walls (Figure 2B). These epidermises are covered with a flat and somewhat thick cuticle (Figures 2a and 2a'). The non-glandular unicellular trichomes are scattered on the upper and lower surfaces of the epidermis with a protective role (Figures 2B and 2k). The angular collenchyma cells comprise many layers, nearly circular cells, and cellulose walls. However, several layers of collenchyma cells located near the upper and lower epidermis are wood-impregnated (lignified and stained blue) (Figure 2b). The palisade parenchyma is single-row and lies below the upper epidermis, which is made up of columnar cells oriented perpendicular to the leaf surface (Figure 2c). The next layer is the spongy parenchyma, which is made up of irregularly shaped cells (Figure 2d). These regions make up the leaf blade (mesophyll). There are 8-9 vascular bundles folded and located near the upper epidermis (Figure 2e). There are many vascular bundles arranged in rows from the midrib to the leaf blade, with an air cavity (approximately 8-10 air cavities) between the two vascular bundles, but this air cavity gradually disappears towards the leaf blade (Figures 2A and 2f). Each vascular bundle consists of the xylem above and the phloem below, which is covered by a ring of the irregularly-sized sclerenchymatous sheath (Figures 2A, 2C and 2D). The xylem includes 1-2 primary veins and 1-3 secondary veins, which are lignified-polygonal in shape and randomly distributed in each vascular bundle (Figure 2h). The phloem comprises 8-10 layers with cellulose-curved polygonal cells (Figure 2i). The sclerenchymatous sheath comprises 1-3 layers above the xylem and 3-5 layers below the phloem with lignified-polygonal cells (Figure 2g). Additionally, oil cells are scattered throughout the parenchymatous leaf (Figures 2b' and 2j).

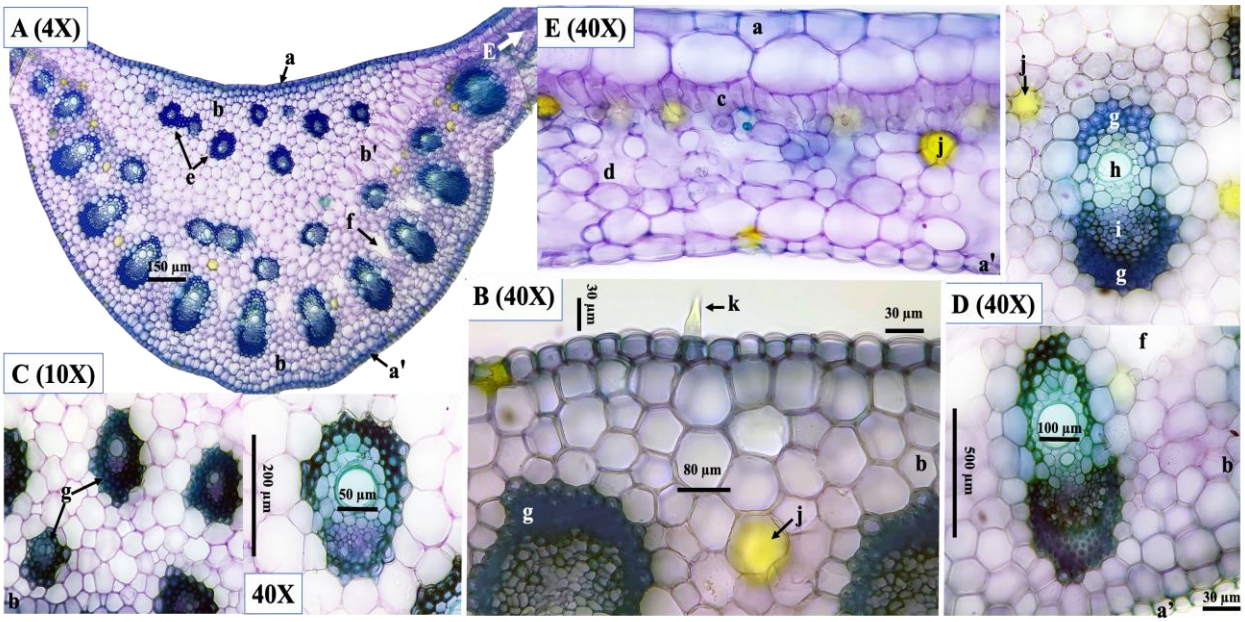

Figure 2. The features of cross-sectioned leaves of *C. vietnamense* (with magnifications 4X, 10X, 40X). A. Leaf midrib. B. Part of the upper leaf midrib. C. Vascular bundles and upper parenchyma tissue. D. Part of the lower leaf midrib. E. Leaf blade (similar in structure to leaf midrib) with palisade parenchyma cells and spongy parenchyma cells. a. Upper epidermis; a'. Lower epidermis; b. Collenchymatous cell; b'. Parenchymatous cell; c. Palisade parenchyma cells; d. Spongy parenchyma cells; e. Vascular bundles (located below the upper epidermis and the center of the midrib); f. Air cavity; g. Sclerenchymatous bundle sheath; h. Xylem; i. Phloem; j. Oil cell; k. Non-glandular unicellular trichomes

Leaf features, such as epidermal cells, oil cells, oleoresin cells, vascular bundles, stomatal index, and the presence or absence of calcium oxalate crystals or trichomes are key anatomical features that are useful in helping to distinguish medicinal species accurately (Osman et al. 2019; Zhao et al. 2022). For example, turmeric (*Curcuma longa* L.) can easily be mixed with sawdust and cornflour to counterfeit this product in the food market. The detection of such ingredients in turmeric products suggests adulteration with non-*Curcuma* species (Osman et al. 2019). A previous review also reported that leaf epidermal cells, midrib vascular bundles, stomatal styles and stomatal indexes, oil cells, mucous cells, calcium oxalate crystals, and trichomes are features that help distinguish species bearing the name *bay leaf* or *bay laurels*, such as *Laurus nobilis* L., *Cinnamomum tamala* (Buch.-Ham.) T.Nees & Eberm., *Litsea glaucescens* Kunth, *Pimenta racemosa* (Mill.) J.W.Moore, *Syzygium polyanthum* (Wight) Walp., and *Umbellularia californica* (Hook. & Arn.) Nutt. (Osman et al. 2019).

In the present study, rhombic-or square-shaped calcium oxalate crystals were found in leaves of *C. vietnamense* as in *Zingiber ellipticum* (S.Q.Tong & Y.M.Xia) Q.G.Wu & T.L.Wu, *Zingiber guangxiense* D.Fang (Zhao et al. 2022), *Curcuma sahuynhensis* Škorničk. & N.S.Lý (Van Chen et al. 2022b), *Curcuma albiflora* Thwaites (Wijayasiriwardena and Premakumara 2016), and *Kaempferia galanga* L. (Paopun 2020). This calcium oxalate crystal form was a component commonly found in the leaves of several genera in Zingiberaceae, such as *Alpinia* (Salasiah and Meekiong 2018), *Amomum*, *Elettaria*, *Zingiber* (Zhao et al. 2022), *Curcuma* (Van Chen et al. 2022b), and *Globba* (Kajornjit et al. 2018). Zhao et al. (2022) also showed that many crystals were commonly found in the veins (i.e., costal epidermal cells) of *Zingiber montanum*. However, these crystals were not found in the veins of *C. vietnamense* leaves.

Non-glandular trichomes are known for their unique function of protecting plants from biotic and abiotic stresses, forming a protective barrier against low humidity, high temperature, and solar radiation as well as preventing insect feeding and oviposition activities (Santos Tozin et al. 2016; Xiao et al. 2017). Trichomes on the leaf surfaces of *C. vietnamense* were unicellular, and are similar to other genera of the family Zingiberaceae, such as *Alpinia*, *Amomum*, *Curcuma*, *Elettaria*, *Kaempferia*, *Hedychium*, and *Zingiber*. Additionally, previous studies have reported that the delicate trichomes were found only on the epidermis of the genera *Boesenbergia* and *Globba*, while the stout trichomes were found only in the genera *Curcuma*, *Alpinia*, *Amomum*, and *Elettaria*. Particularly, stout and delicate trichome types are found in the genera *Kaempferia*, *Hedychium*, and *Zingiber* (Liang et al. 2020; Zhao et al. 2022; Van Chen et al. 2022b).

Small vascular bundles surrounded by rings of sclerenchymatous bundle sheath (8-9 vascular bundles) were randomly scattered under the upper epidermis of the leaf midrib. Air cavities in the leaf midrib were also present in *C. vietnamense* (7-8 air cavities). However, the number of vascular bundles and air cavities also varies in some species that have been recorded in the family Zingiberaceae, such as *Zingiber zerumbet* (L.) Roscoe ex Sm. (1-2 vascular bundles, 4-5 air cavities), *Amomum compactum Roem. & Schult* (absent) (Das et al. 2018), *C. albiflora* (absent, 1-2 air cavities) (Wijayasiriwardene et al. 2016), *Globba marantina* L. (1-2 vascular bundles, 3-4 air cavities) (Roy et al. 2016), *Zingiber officinale* Roscoe (1-2 vascular bundles, 5-6 air cavities) (Liu et al. 2020), *Distichochlamys citrea* M.F.Newman (1-2 vascular bundles, 13-14 air cavities) (Van Chen et al. 2022a), and *Curcuma sahuynhensis* Škorničk. & N.S.Lý (absent, 12-13 air cavities) (Van Chen et al. 2022b). These features distinguish *C. vietnamense* from other species in the family Zingiberaceae.

The adaxial epidermal cells were always more regularly arranged than the abaxial (Figures 3A and 3C). The adaxial epidermis was usually composed of elongated-polygonal cells with a length (L) approximately 1.7 times longer than the width (W). Similarly, the abaxial epidermis was also usually composed of elongated-polygonal cells with a length (L) approximately 1.5 times longer than the width (W). The sizes (L × W) of adaxial and abaxial epidermal cells were 34.20±1.30 × 18.40±1.14 μm and 37.40±2.79 × 24.80±2.17 μm, respectively. The costal epidermal cells consist of two continuously elongated layers, usually smaller, with longitudinally elongated-polygonal cells (Figure 3g).

The stomata type is tetracytic with four subsidiary cells (Figures 3B and 3D), i.e. two lateral subsidiary cells (Figure 3b) and two terminal subsidiary cells (Figure 3c) around the stoma (Figure 3). In other words, the stomatal apparatus consists of guard cells (reniform, Figure 3a) located parallel to the stomata pore (Figure 3d) and lateral subsidiary cells (subtriangular) forming an ellipse (Figures 3a and 3b), while the terminal subsidiary cells (Figure 3c) were located perpendicular adjacent to the stomata poles (Figure 3d) and parallel to the elongated-hexagonal epidermal cells (Figure 3f) with the thickened inner wall of the guard cells (Figure 3e). In addition, the number of stomata on the lower surface is more than on the upper surface of the leaf (Figures 3A, 3B, 3C, and 3D). On the upper surface of the leaf, only very few stomata were observed. Therefore, the stomatal index is calculated for the lower surface of the leaf, i.e., the stomatal index on the abaxial surface found in *C. vietnamense* ($SI_{abaxial}$ = 8.81±0.55%) is also larger than the upper surface of the leaf ($SI_{adaxial}$ = 0.1±0.06%). Furthermore, calcium oxalate crystals were usually rhombic and square shapes. These crystals were scattered and visible in the cells (Figure 3h).

Stomata are cellular breathing pores on the leaf surface with the function of opening and closing to absorb CO_2 and restrict water loss due to transpiration (Nunes et al. 2020). In this study, both adaxial and abaxial surfaces of *C. vietnamense* leaves have the tetracytic type of stomata, specifically found in various species such as *Alpinia purpurata* (Vieill.) K.Schum., *Curcuma aeruginosa* Roxb, *Curcuma heyneana* Valeton & Zijp, *C. longa*, *Curcuma mangga* Valeton & Zijp, *Curcuma zanthorrhiza* Roxb., *Etlingera elatior* (Jack) R.M.Sm., *Kaempferia rotunda* L., *Zingiber officinale* Roscoe, *Zingiber purpureum* Roscoe, *Zingiber ellipticum* (S.Q.Tong & Y.M.Xia) Q.G.Wu & T.L.Wu, and *Wurfbainia compacta* (Sol. ex Maton) Škorničk.

& A.D.Poulsen (Windarsih et al. 2022; Zhao et al. 2022), but different from the paracytic stomatal type reported in *Amomum compactum* Roem. & Schult. (Das et al. 2018), *Curcuma sahuynhensis* Škorničk. & N.S.Lý, and *D. citrea* (Van Chen et al. 2022a, 2022b).

Our results show that the stomatal index on the abaxial surface of *C. vietnamense* leaves (8.81±0.55%) can be significantly distinguished from other species of Zingiberaceae, such as *E. elatior* (30.25±3.34%), *Z. purpureum* (19.11±2.79%), *C. longa* (16.34±1.44%), *K. rotunda* (15.71±2.70%), *A. purpurata* (14.48±3.26%), *W. compacta* (14.22±1.69%), *C. zanthorrhiza* (13.82±2.29%), *Z. ellipticum* (3.67±0.95%), *Zingiber lingyunense* D. Fang (4.74±0.96%), *Zingiber tuanjuum* Z.Y.Zhu (5.86±0.73%), and *Zingiber xishuangbannaense* S.Q.Tong (5.35 ± 0.28%) (Windarsih et al. 2022; Zhao et al. 2022). Similarly, the stomatal index on the adaxial surface of *C. vietnamense* leaves was the lowest (0.1±0.06%) compared with other species, such as *Z. purpureum* (6.97±1.90%), *K. rotunda* (5.14±1.46%), *C. longa* (4.50±1.51%), *C. zanthorrhiza* (3.90±1.30%), *C. mangga* (3.10±0.84%), *W. compacta* (2.46±0.78%), *Z. montanum* (2.87±0.90%), *Zingiber zerumbet* (2.60±0.51%), and *Z. xishuangbannaense* (1.52±0.43%) (Windarsih et al. 2022; Zhao et al. 2022). Segev et al. (2015) and Windarsih et al. (2022) suggested that plants with a lower stomatal index would lead to a lower net photosynthetic rate and vice versa, i.e., the stomatal index correlates with the net rate of photosynthesis. In addition, Segev et al. (2015) also found that the stomatal index is different among species of various genera and families. It demonstrated that the number of stomata in the abaxial epidermis is greater than that in the adaxial epidermis of *C. vietnamense* leaves as our results.

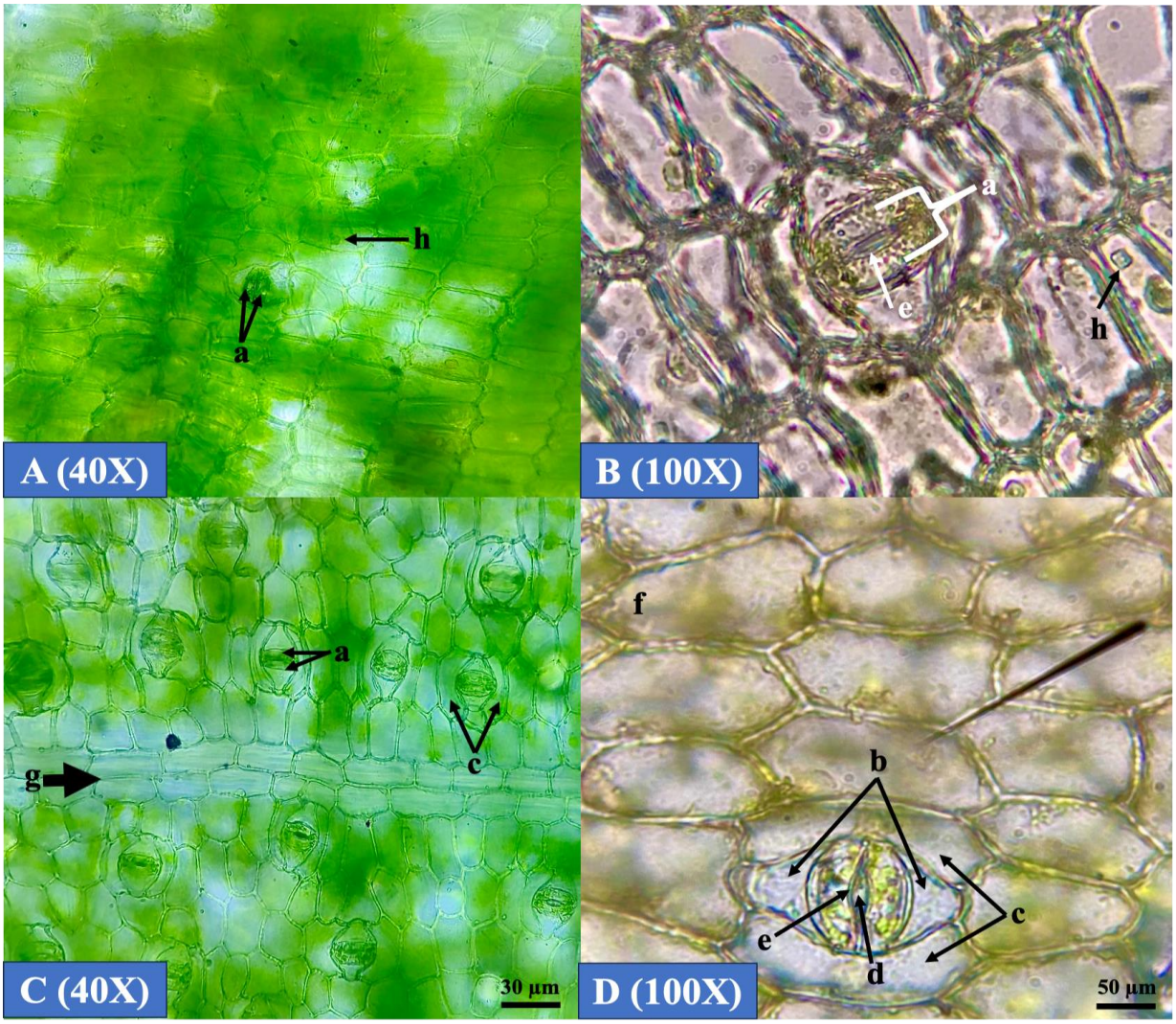

Figure 3. Epidermis with stomata of *C. vietnamense* (with magnifications 40X and 100X). A, B. Upper surface view of the epidermis with stoma closed. C, D. Lower surface view of the epidermis with stoma open. a. Guard cells; b. Lateral subsidiary cells; c. Terminal subsidiary cells; d. Stomatal pore; e. Thickened inner wall of the guard cells; f. Epidermal cells; g. Costal epidermal cells; h. Calcium oxalate crystals (rhombic or square shapes)

Roots

The cross-section of the roots is nearly round and is divided into two distinct regions, namely the cortex area (which accounts for 2/3 of the cross-section) and the pith area (which accounts for 1/3 of the cross-section) (Figure 4A). From the outside to the inside, the cortex area consists of the following layers of epidermis (Figure 4a), exodermis (Figure 4b), suberized hypodermal cells (Figure 4c), and parenchymatous cells of the outer and inner cortex (Figures 4B, 4d, and 4e). The suberized hypodermal cells comprise 7-9 layers, polygonal cells, cork-impregnated walls, and a random arrangement (Figure 4c). The outer parenchymatous cells comprise about 12-13 layers; the cells are nearly round, polygonal cells, with thin cellulose walls and a random arrangement (Figure 4d). The inner parenchymatous cells consist of 4-5 layers; the cells are nearly rectangular, thin cellulose walls, arranged in radial and concentric rings (Figure 4e). Additionally, the parenchyma cell regions of the outer and inner cortex show that there is an empty polygonal or triangular intercellular space (Figure 4f). The pith zone, which connects from the last cell layer of the inner parenchymatous cell region, includes the endodermis, pericycle, vascular bundle (xylem and phloem), parenchyma rays, and parenchymatous pith (the outer domain and the inner domain) (Figure 4C). The endodermis is a single-layer "U"-shaped and polygonal cell (Figure 4g). The next layer is the pericycle, consisting of a single layer, polygonal cells, and cellulose walls (Figure 4h). The next structure comprises 34-36 bundles of protoxylem interspersed with 35-36 phloem bundles and arranged in a ring (Figures 4j, 4i, and 4k). Each bundle of protoxylem has 3-5 vessels, polygonal protoxylem vessels, wood-impregnated walls, and radial differentiation (Figure 4j). Metaxylem consists of 18-20 polygonal-shaped bundles, impregnated walls with wood (Figure 4i), and is 4-5 times larger than that of the protoxylem (Figures 4j and 4i). Phloem has polygonal cells, and cellulose walls, arranged in clusters (Figure 4k). The parenchymatous ray consists of 1-2 rows of polygonal cells, cellulose walls, or impregnated with wood (Figure 4l). The parenchymatous stele is divided into two areas: the outer area (around the metaxylem) is multi-layered, with polygonal cells, and the walls are impregnated with wood and arranged in dense sclerenchymatous conjunctive tissues (Figure 4m); the inner region contains several layers of parenchymatous tissue, nearly circular cells, cellulose walls, and random arrangement with intercellular spaces (Figure 4n). Essential oil-secreting cells are scattered throughout the cortical parenchyma cells (Figure 4o).

Generally, the epidermis layer, exodermis layer, suberized hypodermal cells, and the outer cortex region of *C. vietnamense* are similar to the genera *Alpinia* (e.g., *Alpinia calcarata* (Andrews) Roscoe, *Alpinia vittata* W.Bull, *Alpinia smithiae* M.Sabu & Mangaly, and *A. purpurata*), *Amomum* (e.g., *Amomum aculeatum* Roxb.), *Curcuma* (e.g., *Curcuma aromatica* Salisb., *C. longa*, and *C. sahuynhensis*), *Zingiber* (e.g., *Z. officinale*, *Z. zerumbet*, and *Z. purpureum*), *Hedychium* (e.g., *Hedychium coronarium* J.Koenig, *Hedychium coccineum* Buch.-Ham. ex Sm., and *Hedychium flavescens* Carey ex Roscoe), *Etlingera* (e.g., *E. elatior*), *Globba* (e.g., *Globba schomburgkii* Hook.f. and *G. marantina*), and *Kaempferia* (e.g., *Kaempferia elegans* Wall., *K. galanga*, and *K. rotunda*) (Uma and Muthukumar 2014; Gevú et al. 2014; Roy et al. 2016; Van Chen et al. 2022b). However, tissues of the inner cortex region of *C. vietnamense* are characterized by polygonal or triangular intercellular spaces (similar to *Curcuma amada* Roxb., *D. citrea*, *E. elatior*, *Z. officinale*, *Z. purpureum*, and *Z. zerumbet*), but different from *C. sahuynhensis* (Van Chen et al. 2022b), *Curcuma zedoaria*, *C. aromatica*, *C. longa*, *K. galanga* (linear intercellular spaces) and *G. schomburgkii* (lack of intercellular spaces) (Uma and Muthukumar 2014). Furthermore, stellate cells were not found in the cortical parenchyma of *C. vietnamense* but were observed only in *H. coronarium* (Gevú et al. 2014).

The uniseriate endoderm comprises "U"-shaped thickening walls and dividing endodermal cells forming radial rows of cortical parenchyma cells. These structures were observed in the roots of *C. vietnamense*, a feature similar to that of the genera *Alpinia*, *Amomum*, *Curcuma*, *Etlingera*, and *Renealmia*, as previously reported by Uma and Muthukumar (2014) and Gevú et al. (2014). The exodermis with thin and lightly suberized hypodermal cells including 4 to 6 layers has been recorded in different species, such as *A. purpurata*, *A. zerumbet*, *C. longa*, *C. zedoaria*, *E. elatior*, *Etlingera fulgens* (Ridl.) C.K.Lim, *H. coronarium*, *Renealmia chrysotricha* Petersen, *Z. officinale*, *Zingiber spectabile* Griff. (Gevú et al. 2014), *D. citrea*, and *C. sahuynhensis* (Van Chen et al. 2022a, 2022b). However, the suberized hypodermal cells consist of 7-9 layers with polygonal cells, and wood-impregnated walls are also recorded in *C. vietnamense* roots.

Rhizomes

The cross-section of the rhizome in *C. vietnamense* is nearly circular. The epidermis has a single layer, polygonal cells, cellulose walls, and a flat, thin cutin layer (Figure 5a). The cortical parenchyma cell has many layers, the parenchymatous cells are polygonal and nearly round (Figure 5b), and the cellulose wall is thin and randomly arranged with the polygonal intercellular space (Figure 5b'). Closed vascular bundles (i.e., bundles of vessels with a sclerenchymatous bundle sheath ring) are large, small, and scattered in the parenchymatous cell of the cortex (Figure 5c). The sclerenchymatous bundle sheath ring consists of 2-3 layers, polygonal cells, and wood-impregnated walls (Figure 5d). Closed vascular bundles (Figure 5c') below the ring of sclerenchymatous conjunctive tissues (Figure 5e) (i.e., belonging to the pith region of the rhizome), arranged upside-down on many rings, the size gradually increased from the ring of sclerenchymatous conjunctive tissues inward. Especially, each closed vascular bundle consists of the phloem above, the xylem below, and the sclerenchymatous bundle sheath around the phloem-xylem. Phloem is arranged randomly, polygon-shaped cells with cellulose-impregnated and curved walls (Figure 5f). The protoxylem comprises 2-3 polygonal vessels with wood-impregnated walls (Figure 5g). Metaxylem consists of 3-5 polygonal vessels, wood-impregnated walls, 1.5-2 times larger than protoxylem (Figure 5h). The

sclerenchymatous bundle sheath comprises 1-2 layers, polygonal cells, and impregnated walls with wood substance (Figure 5d'). The parenchymatous tissue of the stele consists of many layers; the parenchymatous cells are nearly circular and randomly arranged with polygonal or triangular intercellular spaces (Figure 5i). Casparian strips in endodermis and pericycle are especially difficult to distinguish because they have been structurally altered to form rings of walls-impregnated sclerenchymatous conjunctive tissues with a blue-tinted woody substance. Essential oil-secreting cells are scattered throughout the parenchymatous cells of the cortex and stele regions (Figure 5j).

In general, our results explained the similar anatomical structure of the *C. vietnamense* root including the epidermis layer, cortex region (e.g., parenchymatous cells, oil cells), and pith region (e.g., parenchymatous cells, vascular bundles, oil cells) compared with the anatomical structure of the rhizome. However, the vascular bundles surrounded by rings of sclerenchymatous bundle sheath are scattered throughout the rhizome, and the absence of suberized hypodermal cell layers in the cortex region are distinguishing features from the roots of this species. In contrast, the sclerenchymatous conjunctive tissue layers and parenchymatous rays in the pith region of the root are also distinguishing features from the cortex region of the rhizome (i.e., parenchymatous cells) as analyzed in this study.

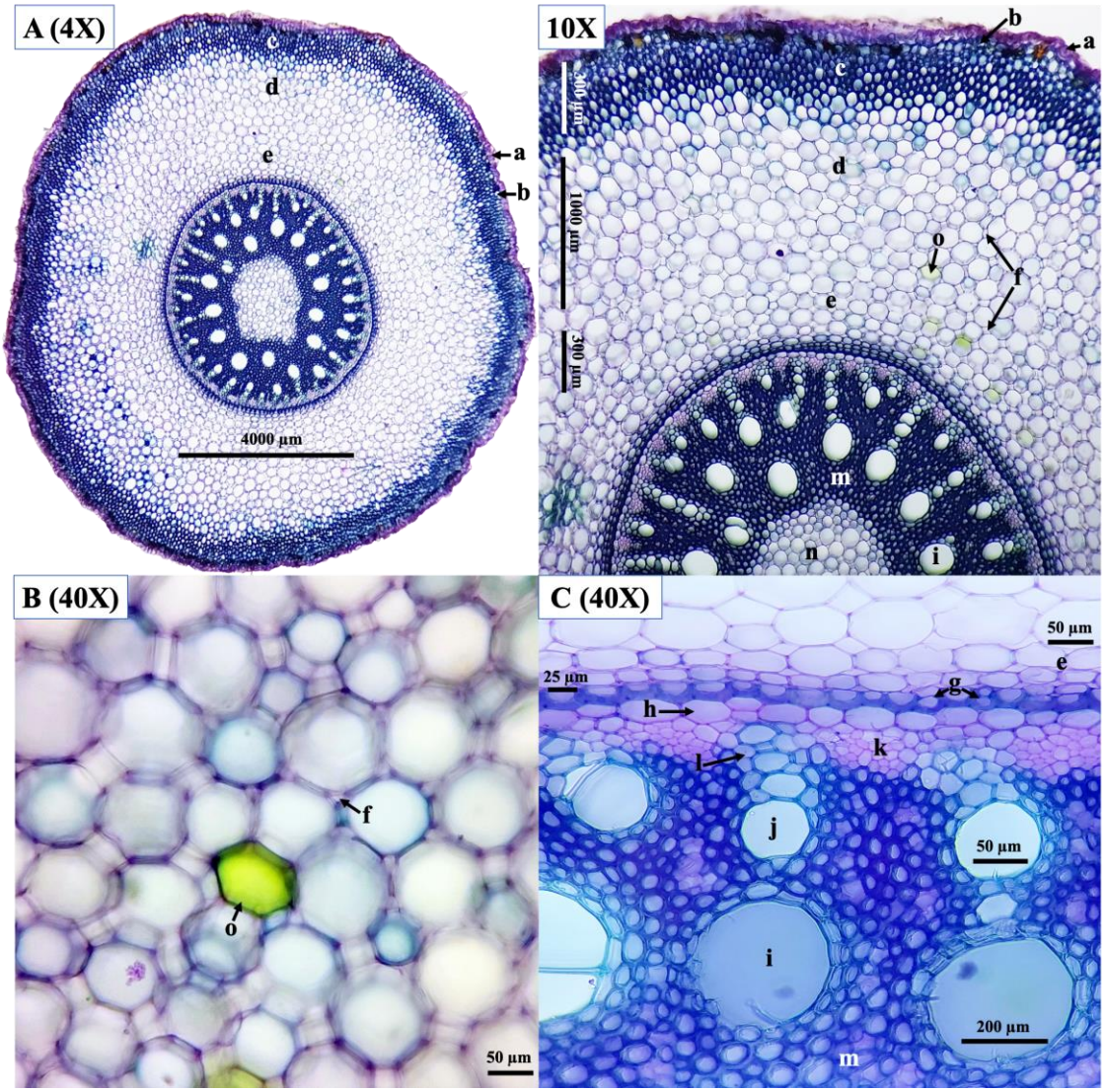

Figure 4. The features of the cross-sectioned root of *C. vietnamense* (with magnifications 4X, 10X, 40X). A. Cross section of root; B. Parenchymatous tissue of the root cortex with oil cell; C. The pith/stele area; a. Epidermis; b. Exodermis; c. Suberized hypodermal cells; d. Parenchymatous cells of the outer cortex; e. Parenchymatous cells of the inner cortex; f. Polygonal or triangular intercellular spaces; g. "U" shape thickening in endodermis and endodermis cells in the division; h. Pericycle; j. Protoxylem; i. Metaxylem; k. Phloem; l. parenchymatous ray; m. Sclerenchymatous conjunctive tissues; n. Parenchymatous pith; o. Oil cell

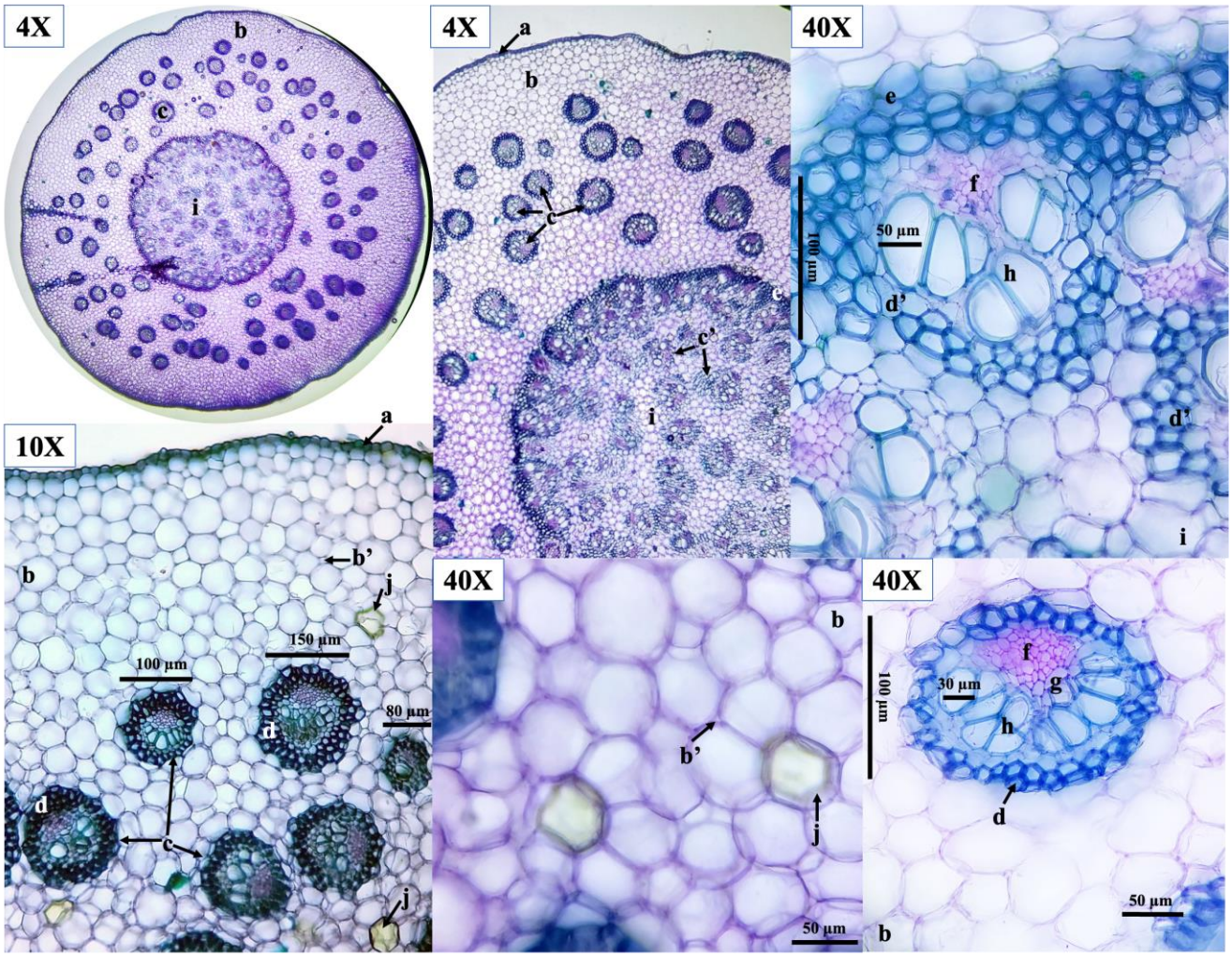

Figure 5. The features of cross-sectioned rhizome of *C. vietnamense* (with magnifications 4X, 10X, 40X). a. Epidermis with thin cutin layer; b. Parenchymatous cells of the cortex region; b'. Polygonal or triangular intercellular spaces; c. Closed vascular bundles of the cortex region; d. Sclerenchymatous bundle sheath of the cortex region; d'. Sclerenchymatous bundle sheath of the pith region; e Sclerenchymatous conjunctive tissues; f. Phloem; g. Protoxylem; h. Metaxylem; i. Parenchymatous cells with intercellular spaces of the pith region; j. Oil cell

The anatomical structure of the *C. vietnamense* rhizome is similar to other species of the family Zingiberaceae (e.g., *Alpinia galanga*, *C. sahuynhensis*, *C. aromatica*, *C. aeruginosa*, *C. zedoaria*, *C. albiflora*, *C. caesia*, *C. longa*, *D. citrea*, and *Z. officinale*) including the epidermis, cortex region, and pith region (Roy et al. 2013; Anu et al. 2020; Liu et al. 2020; Van Chen et al. 2022a, 2022b). However, the multilayered hypodermis was observed in the above species, but was absent in *C. vietnamense* rhizomes. Moreover, the absence of multilayered hypodermis in *C. vietnamense* rhizomes was similar to that in *Z. zerumbet* rhizomes (Roy et al. 2013). For various species of the family Zingeberaceae (e.g., *Alpinia purpurata*, *A. zerumbet*, *C. longa*, *C. zedoaria*, *C. sahuynhensis*, *D. citrea*, *E. elatior*, *Etlingera fulgens*, *H. coronarium*, *R. chrysotricha*, *Z. officinale*, and *Z. spectabile*), the number of protoxylem and metaxylem elements per vascular bundle varies as in previous reports (Gevú et al. 2014; Van Chen et al. 2022a, 2022b). Furthermore, the delineation of the cortex and pith regions is marked by the presence of casparian strips in the endodermis (Gevú et al. 2014; Van Chen et al. 2022a, 2022b). However, the presence of the endoderm with Casparian strips in the rhizome of *C. vietnamense* is not explicit, but it tends to arrange randomly to form a circular band characterized by walls-impregnated sclerenchymatous conjunctive tissues with a blue-tinted woody substance. Additionally, previous studies revealed that the vascular bundle system is an irregular and randomly arranged structure. Moreover, vascular bundles in the pith region are more developed and present in larger numbers than in the cortex region (e.g., *A. purpurata*, *A. zerumbet*, *C. longa*, *C. zedoaria*, *C. sahuynhensis*, *D. citrea*, *E. elatior*, *E. fulgens*, *H. coronarium*, *R. chrysotricha*, *Z. officinale*, and *Z. spectabile*) (Gevú et al. 2014; Van Chen et al. 2022a, 2022b). In contrast, the number of vascular bundles in the cortex region (approximately 85±5 vascular bundles) is larger numbers as compared to the pith region (approximately 65±5 vascular bundles) which has been observed in the rhizome of *C. vietnamense*. These features may help

distinguish *C. vietnamense* and other species of the family Zingiberaceae.

Based on the micro-morphological analysis, oil cells were found in *C. vietnamense* leaves more than in rhizomes. This is consistent with the results of hydrolyzed distillate oil yield from leaves (0.43%) and rhizomes (0.37%) from *C. vietnamense* reported by Nguyen et al. (2023). Rhizomes of most species within the family Zingiberaceae (e.g., *Amomum tsao-ko*, *Z. officinale*, *Z. montanum*, *Z. zerumbet*, and *C. sahuynhensis*) are commonly used in folklore for the flavor, color, aroma of food and the treatment of diseases including stomach problems, ulcers, gastrointestinal disorders, nausea, vomiting, sore throat, cough, common cold, bruises, wounds, rheumatism, muscular pains, atherosclerosis, and anti-cancer (Shukla and Singh 2007; Sharifi-Rad et al. 2017; Van Chen et al. 2022b; He et al. 2023). Nguyen et al. (2023) reported that eucalyptol (49.49% in leaves oil, 40.47% in rhizomes oil), limonene (26.20% in leaves oil, 18.74% in rhizomes oil), α-pinene (4.91% in leaves oil, 3.60% in rhizomes oil), and α-phellandrene (3.77% in leaves oil, 3.30% in rhizomes oil) were the main constituents in the essential oil of *C. vietnamense* leaves and rhizomes. It shows that the rhizome is a commonly used part. Still, the leaves of *C. vietnamense* are also a source of raw materials that need to be developed to serve the future promising pharmaceutical and cosmetic industries.

The study of micro-morphological characteristics of roots and leaves serves as a theoretical basis to determine the phylogenetic and evolutionary relationships among species and genera (Tang et al. 2010; Wu et al. 2014; Van Chen et al. 2022a, 2022b). This work describes the leaves, roots, and rhizomes of micro-morphology and anatomy of *C. vietnamense* for the first time. This method is still valuable as a contribution to plant taxonomy, from which it is possible to accurately identify plant species, such as correctly identifying of *C. vietnamense*.

Powder

Root and rhizome powder

The root and rhizome powder in *C. vietnamense* has a yellow-brown color (Figure 6A), a light spicy taste, and an aroma-specific odor. Based on microscopic observation, numerous fragments of yellow-brown epidermis cells are present with elongated-polygonal and irregular shapes (Figure 6B) and the polygonal fragments of parenchymatous cells (Figure 6C). Numerous starch granules are ovoid, oval, egg-shaped or pear-shaped (4.0-10 µm in diameter). The hilum of starch granules is generally short-streaked or absent (the hilum is at the large end of the seed ovoid), and the concentric lines are not obvious (Figure 6D). In addition to the starch granules, many calcium oxalate crystals are visible in the parenchymatous cells (Figures 6D and 6E). Spiral vessels (Figure 6G) and reticulate vessels (Figure 6H) are fragments of xylem vessels thickening. In the observation field, thick-walled crystal fiber (Figure 6F) and red-brown oleoresin masses are also found (Figures 6B, 6G, and 6H, blue arrows).

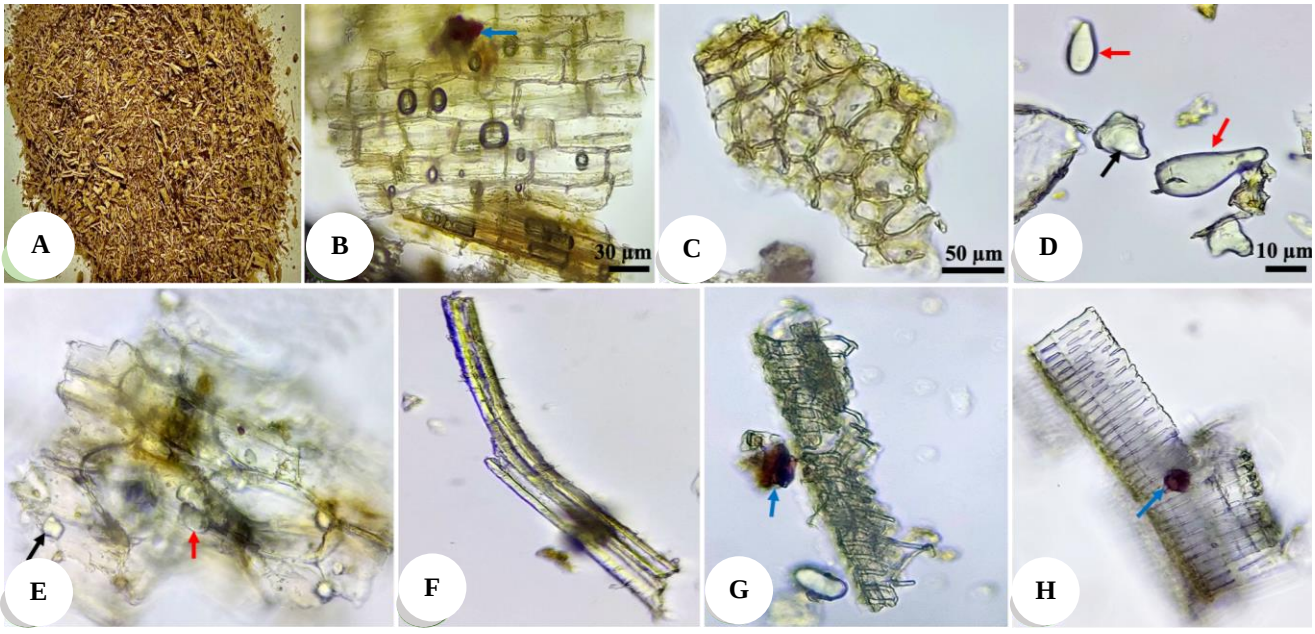

Figure 6. The features of *C. vietnamense* root and rhizome powders. A. Root and rhizome powders. B. Epidermal cells with red-brown oleoresin masses (blue arrow). C. Parenchymatous cells. D. Calcium oxalate crystals (solid shape, black arrow) and starch granules (egg-shaped or pear-shaped, red arrows). E. Parenchymatous cells with starch granules (red arrow) and calcium oxalate crystals (black arrow). F. Thick-walled crystal fiber. G. Spiral xylem vessel with red-brown oleoresin masses (blue arrow). H. Reticulate xylem vessel with red-brown oleoresin masses (blue arrow)

Leaf powder

The dried powder leaf has a slightly green color, an aromatic odor, and a lightly spicy taste (Figure 7A). Microscopically, the leaf powder is characterized by polygonal fragments of epidermis and contains tetracytic stomata, and costal epidermal cells (Figure 7B). The numerous fragments of green epidermal cells with thin walls (Figure 7C), the polygonal fragments of parenchymatous cells (Figure 7D), fragments of thick spiral xylem vessel (Figure 7e), thick-walled crystal fiber (Figure 7F), and calcium oxalate crystals (solid and square shapes) (Figures 7G and 7H) are also found in leaf powder. The ingredients found in fresh leaves and leaf powder are similar in composition. However, the upper and lower epidermises are difficult to locate components in the leaf powder.

Osman et al. (2019) reported the organoleptic method using the senses of sight, smell, or taste to observe the characteristic color, smell, or taste of spices or herbs. However, the mixture of deliberate or unintentional adulteration of these powders makes it difficult to distinguish the correct medicinal powders; therefore, this method provides rapid sample visualization, and it is often combined with microscopy for preliminary examination of the identity and purity of spices as well as raw powders (Alamgir 2017; Osman et al. 2019). Microscopic descriptions of powdered material assist in accurately identifying of medicinal herbs (WHO 2011; Alamgir 2017; Srivastava and Misra 2018; Osman et al. 2019). Additionally, based on the features of plant tissue, the microscope is a simple and quick tool for testing the purity of raw powders (Wijayasiriwardena and Premakumara 2012; Osman et al. 2019; Van Chen et al. 2022b).

The rhizome and leaf powders of *C. vietnamense* were studied in detail by microscopy to highlight important anatomical features. the main characteristics of *C. vietnamense* powdered rhizomes are those of epidermal cells, parenchymal cells, starch granules, xylem vessels, crystal fibers, calcium oxalate crystals, and oleoresin. Diagnostic identification features of *C. vietnamense* were reticulate xylem vessels and pear-shaped starch grains in rhizome powder compared to that of *D. citrea* (Van Chen et al. 2022a), *C. sahuynhensis* (Van Chen et al. 2022b), *A. calcarata* and *A. galanga* (Mathew et al. 2014). Particularly, solid-or square-shaped calcium oxalate crystals were found only on *C. vietnamense* rhizome powder and were not present in the rhizome powder of *A. calcarata* (Wijayasiriwardena and Premakumara 2012; Mathew et al. 2014), *C. sahuynhensis* (Van Chen et al. 2022b), *C. longa* (Amel 2015), *Z. officinale* (Abdulrahaman et al. 2015; Ahmed and Kumar 2022), *D. citrea* (Van Chen et al. 2022a), and *G. marantina* (Roy et al. 2016). Similarly, the major components found in the leaf powder sample were the epidermal cells, parenchymal cells, xylem vessels, crystal fibers, and calcium oxalate crystals. Nonetheless, the red-brown oleoresin masses are not found in the *C. vietnamense* leaf powder, a result similar to that of *A. calcarata* and *A. galanga* (Mathew et al. 2014). However, these oleoresin masses are found in *G. marantina* (Roy et al. 2016), *D. citrea* (Van Chen et al. 2022a), and *C. sahuynhensis* leaf powders (Van Chen et al. 2022b). Therefore, detecting these oleoresins in *C. vietnamense* leaf powders indicates adulteration with other species.

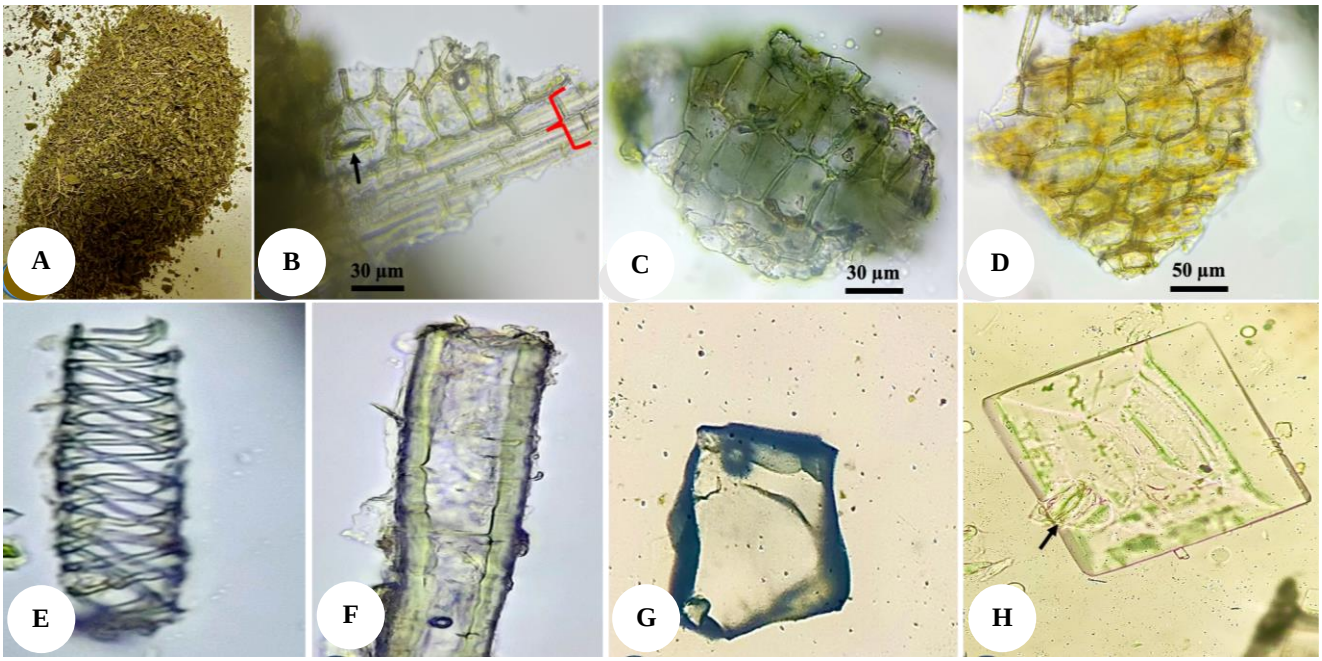

Figure 7. The features of dried leaf powder of *C. vietnamense* (with magnifications 40X): A. Leaf powder. B. Epidermal surface with stomata (*black arrow*) and costal epidermal cells (*red arrow*). C. Fragment of epidermal cells. D. Fragment of parenchymatous cells. E. Spiral xylem vessel. F. Thick-walled crystal fiber. G. Calcium oxalate crystal (solid shape). H. Calcium oxalate crystal (square shape) and fragment of stomata (*arrow*)

As a result of the study of *C. vietnamense* rhizome and leaf powders composition, it can be suggested that the absence of epidermal and parenchymatous cells, solid-shaped calcium oxalate crystals, thick-walled crystal fiber, egg-shaped or pear-shaped starch granules, spiral xylem vessel, reticulate xylem vessel, and red-brown oleoresin masses in the rhizome powder samples, as well as the absence of epidermal and parenchymatous cells, spiral xylem vessel, solid-shaped and square-shaped calcium oxalate crystals, thick-walled crystal fiber in the leaf powder samples; all of these ingredients will aid in the identification of deliberate or unintentional adulteration with the raw powder.

In general, macroscopic observation is a method that has long been used to validate and evaluate the quality of herbal drugs (WHO 2011; Zhao et al. 2011; Alamgir 2017). These macroscopic analyses involve phenotypic characteristics that may vary under different conditions such as the growing environment, the time of harvest, the method of standardization of raw materials, or the processing or storage conditions of herbal drugs (Zhao et al. 2011). Identifying the origin of raw materials and herbal medicines is especially difficult. Faced with the disadvantages of macroscopic analysis, microscopic analysis of the plant cross-sections or powders of medicinal herbs by microscopy has the advantage of allowing analysis at the cellular level and is more suitable for the identification of species or the verification of adulteration (Alamgir 2017; Srivastava and Misra 2018; Muyumba et al. 2021). It is also the method used when drugs are presented in powder form to check for mixing of species for fraudulent purposes (Zhao et al. 2005; Wijayasiriwardena and Premakumara 2012; Muyumba et al. 2021).

In conclusion, the anatomical characteristics of leaves, roots, and rhizomes and the micro-morphological characteristics of the raw powder of *C. vietnamense* were reported for the first time in the present study. The comparative microscopic observations of *C. vietnamense*'s cross-sectioned roots, rhizomes, leaves, and crude powder with other Zingiberaceae species, such as *A. galanga*, *C. sahuynhensis*, *C. zedoaria*, *C. caesia*, *D. citrea*, *Z. officinale*, etc., revealed that many of these micromorphological features are homologous. Accordingly, the root and rhizome structures consist of the epidermis, the cortex region, and the stele region, which are relatively similar. The powder rhizome characteristics (the epidermal cells with red-brown oleoresin masses, fragments of parenchyma, calcium oxalate crystals, starch granules, thick-walled crystal fiber, fragments of spiral xylem vessel, fragments of reticulate xylem vessel) and the powder leaf characteristics (fragment of epidermal cells, fragment of parenchymatous cells, fragments of spiral xylem vessel, thick-walled crystal fiber, calcium oxalate crystal) are commonly found in the observation field. This specific information has been well constructed and documented to constitute a summary monograph of macro- and micro-morphological characteristics, an important source of reliable information for accurately identifying this species, namely *C. vietnamense*. The present study revealed an easy technique to identify *C. vietnamense*, medicinal plant material, under a microscope. This method can also be used to detect the degree of impurity in medicinal plant raw materials.

ACKNOWLEDGEMENTS

The authors thank the partial facility support of ChenPharm's Lab for this study. This research was funded by Nguyen Tat Thanh University for Science and Technology Development under grant number 2023.01.23/ HD-KHCN.

REFERENCES

Abdulrahaman AA, Taiwo MO, Oladele FA. 2015. Phytopharmaceutical potential and microscopic analysis of rhizomes of *Curcuma longa* and *Zingiber officinale* (Zingiberaceae). Ann West Univ Timiș Ser Biol 18 (2): 73-86.

Ahmed SS, Kumar R. 2022. Pharmacognostical standardization of *Cassia auriculata*, *Centella asiatica* and *Zingiber officinale*. J Med Pharm Allied Sci 11 (5): 5227-5231. DOI: 10.55522/jmpas.V11I5.4060.

Alamgir ANM. 2017. Pharmacognostical botany: Classification of Medicinal and Aromatic Plants (MAPs), botanical taxonomy, morphology, and anatomy of drug plants. In: Rainsfors KD (ed) Therapeutic Use of Medicinal Plants and Their Extracts: Volume 1. Progress in Drug Research 73: 177-293. Springer, Cham. DOI: 10.1007/978-3-319-63862-1_6.

Amel B. 2015. Microscopic analysis of *Curcuma longa* L. using multivariate test. Intl J Pharmacol 2 (4): 173-177. DOI: 10.13040/IJPSR.0975-8232.

Anu S, Navas M, Dan M. 2020. Morpho-anatomical characterisation of the rhizomes of ten species of *Curcuma* L. (Zingiberaceae) from South India. J Spices Aromat Crops 29 (1): 38-47. DOI: 10.25081/josac.2020.v29.i1.6243.

Boer HD, Newman M, Poulsen AD, Droop AJ, Fér T, Thu Hiền LT, Hlavatá K, Lamxay V, Richardson JE, Steffen K, Leong-Škorničková J. 2018. Convergent morphology in *Alpinieae* (Zingiberaceae): Recircumscribing *Amomum* as a monophyletic genus. Taxon 67 (1): 6-36. DOI: 10.12705/671.2.

Das A, Pal KK, Nag S. 2018. Anatomy, micromorphology and histochemical localization of different phytochemicals of two medicinally important taxa of the family Zingiberaceae. Res J Life Sci Bioinform Pharm Chem Sci 4 (1): 190-198. DOI: 10.26479/2018.0401.16.

Gevú KV, Da Cunha M, Barros CF, Pereira SM, Lima HRP. 2014. Structural analysis of subterranean organs in Zingiberaceae. Plant Syst Evol 300 (5): 1089-1098. DOI: 10.1007/s00606-013-0947-y.

He G, Yang SB, Wang YZ. 2023. The potential of *Amomum tsao-ko* as a traditional Chinese medicine: Traditional clinical applications, phytochemistry and pharmacological properties. Arab J Chem 16 (8): 104936. DOI: 10.1016/j.arabjc.2023.104936.

Holttum RE. 1950. The Zingiberaceae of the Malay Peninsula. Gard Bull Singapore 13: 1-250.

Kajornjit P, Saensouk S, Saensouk P. 2018. Pollen morphology and leaf anatomy of genus *Globba* in Thailand. Sci Asia 44 (3): 146-161. DOI: 10.2306/scienceasia1513-1874.2018.44.146.

Lamxay V, Newman MF. 2012. A revision of *Amomum* (Zingiberaceae) in Cambodia, Laos and Vietnam. Edinb J Bot 69 (1): 99-206. DOI: 10.1017/S0960428611000436.

Le Breton TD, Zimmer HC, Gallagher RV, Cox M, Allen S, Auld TD. 2019. Using IUCN criteria to perform rapid assessments of at-risk taxa. Biodivers Conserv 28: 863-883. DOI: 10.1007/s10531-019-01697-9.

Liang H, Zhang Y, Deng J, Gao G, Ding C, Zhang L, Yang R. 2020. The complete chloroplast genome sequences of 14 *Curcuma* species: Insights into genome evolution and phylogenetic relationships within Zingiberales. Front Genet 11: e802. DOI: 10.3389/fgene.2020.00802.

Liu H, Specht CD, Zhao T, Liao J. 2020. Morphological anatomy of leaf and rhizome in *Zingiber officinale* Roscoe, with emphasis on secretory structures. Hort Sci 55 (2): 204-207. DOI: 10.21273/HORTSCI14555-19.

Luu DNA, Bui VH, Luu DC, Nguyen QH, Trinh XT, Thanh TN. 2021. *Conamomum pierreanum* (Gagnep.) Skornick. & AD Poulsen (Zingiberaceae), a new record for the flora of Vietnam. VNU J Sci Nat Scie Technol 37: 41-45. DOI: 10.25073/2588-1140/vnunst.5035.

Ly NS, Hoang TS, Insisiengmay O, Haevermans T, Newman MF. 2022. *Conamomum vietnamense* (Zingiberaceae), a new species from Tay Nguyen, Vietnam. Phytotaxa 531 (2): 129-135. DOI: 10.11646/phytotaxa.531.2.5.

Mathew S, Britto SJ, Thomas S. 2014. Comparative powder microscopical screening of the rhizome and leaf of *Alpinia calcarata* and *Alpinia galanga*. Intl J Pharm Sci Res 5: 1449. DOI: 10.13040/IJPSR.0975-8232.5(4).1449-53.

Ministry of Health. 2017. Vietnamese Pharmacopoeia V. Medical Publishing House, Ha Noi.

Muyumba NW, Mutombo SC, Sheridan H, Nachtergael A, Duez P. 2021. Quality control of herbal drugs and preparations: The methods of analysis, their relevance and applications. Talanta Open 4: 100070. DOI: 10.1016/j.talo.2021.100070.

Nguyen DD, Nguyen NH, Tran TH, Nguyen DK, Thi Nguyen LT. 2023. Limonene and eucalyptol rich essential oils with their antimicrobial activity from the leaves and rhizomes of *Conamomum vietnamense* N.S. Lý & T.S. Hoang (Zingiberaceae). Pharmacia 70 (1): 91-96. DOI: 10.3897/pharmacia.70.e96946.

Nunes TD, Zhang D, Raissig MT. 2020. Form, development and function of grass stomata. Plant J 101 (4): 780-799. DOI: 10.1111/tpj.14552.

Osman AG, Raman V, Haider S, Ali Z, Chittiboyina AG, Khan IA. 2019. Overview of analytical tools for the identification of adulterants in commonly traded herbs and spices. J AOAC Intl 102 (2): 376-385. DOI: 10.5740/jaoacint.18-0389.

Paopun Y. 2020. Calcium oxalate crystals and leaf anatomical characteristics of *Kaempferia galanga* L. J Microsc Microanal Res 33 (1): 28-33. DOI: 10.14456/microsc-microanal-res.2020.7.

POWO. 2023. Plants of the World Online. https://powo.science.kew.org /taxon/urn:lsid:ipni.org:names:37235-1.

Ridley HN.1899. The Scitamineae of the Malay Peninsula. J Straits Branch Roy Asiat Soc 32: 85-184.

Roy B, Jana BK, Maiti GG. 2013. Morpho-anatomical diversity of the rhizomes of some medicinal and aromatic plants of Zingiberaceae. Intl J Chem Pharm Res 2 (8): 197-203.

Roy S, Acharya RN, Harisha CR, Shukla VJ. 2016. Macro, microscopic and preliminary analytical evaluation of root and leaf of *Globba marantina* Linn.-An extrapharmacopoeial drug of Ayurveda. Indian J Pharm Sci 78 (4): 469-478. DOI: 10.4172/pharmaceutical-sciences.1000141.

Salasiah M, Meekiong K. 2018. Preliminary anatomical study on leaf surfaces of Bornean Zingiberaceae (tribe *Alpinieae*) from northeast Sarawak. Malays Appl Biol 47 (5): 289-293.

Santos Tozin LRD, de Melo Silva SC, Rodrigues TM. 2016. Non-glandular trichomes in Lamiaceae and Verbenaceae species: morphological and histochemical features indicate more than physical protection. N Z J Bot 54 (4): 446-457. DOI: 10.1080/0028825X.2016.1205107.

Segev R, Nannapaneni R, Sindurakar P, Kim H, Read H, Lijek S. 2015. The effect of the stomatal index on the net rate of photosynthesis in the leaves of *Spinacia oleracea*, *Vinca minor*, *Rhododendron* spp., *Epipremnum aureum*, and *Hedera* spp. J Emerg Investig 20: 1-5.

Sharifi-Rad M, Varoni EM, Salehi B, Sharifi-Rad J, Matthews KR, Ayatollahi SA, Rigano D. 2017. Plants of the genus *Zingiber* as a source of bioactive phytochemicals: From tradition to pharmacy. Molecules 22 (12): 2145. DOI: 10.3390/molecules22122145.

Shukla Y, Singh M. 2007. Cancer preventive properties of ginger: A brief review. Food Chem Toxicol 45 (5): 683-690. DOI: 10.1016/j.fct.2006.11.002.

Srivastava S, Misra A. 2018. Quality control of herbal drugs: Advancements and challenges. *In*: Singh B, Peter K (eds). New Age Herbals: Resource, Quality and Pharmacognosy, Springer, Singapore. DOI: 10.1007/978-981-10-8291-7_10.

Tang Y, Liao J, Wu Q. 2010. Analyses of anatomic structure and their systematic significances of Zingiberaceous roots of 28 species in China. Acta Bot Boreal Occid Sin 30 (9): 1821-1833.

Truong LH, Dang TH, Dat NQ, Trung NTQ, Gioi T. 2019. *Conamomum odorum*, a new species of Zingiberaceae from central Vietnam. Academia J Biol 41: 55-59. DOI: 10.15625/2615-9023/v41n3.13671.

Uma E, Muthukumar T. 2014. Comparative root morphological anatomy of Zingiberaceae. Syst Biodivers 12 (2): 195-209. DOI: 10.1080/14772000.2014.894593.

Van Chen T, Tuan ND, Triet NT, An NH, Nguyen PTT, Hai NTT, Nhi NTT, Co NQ, Nhi HTH, Huong HV, Phuong TTB, Nhung NTA. 2022a. Morphological and molecular characterization of *Distichochlamys citrea* M.F. Newman in Bach Ma National Park, Thua Thien Hue Province, Vietnam. Biodiversitas 23 (4): 2066-2079. DOI: 10.13057/biodiv/d230442.

Van Chen T, Lam DNX, Thong CLT, Nguyen DD, Nhi NTT, Triet NT. 2022b. Morphological characters, pharmacognostical parameters, and preliminary phytochemical screening of *Curcuma sahuynhensis* Škorničk. & N.S. Lý in Quang Ngai Province, Vietnam. Biodiversitas 23 (8): 3907-3920. DOI: 10.13057/biodiv/d230807.

WHO. 2011. Quality Control Methods for Medicinal Plant materials. WHO Press, Geneva.

Wijayasiriwardena C, Premakumara S. 2012. Comparative powder microscopy of *Alpinia calcarata* Roscoe and *Alpinia galanga* (Linn.) Willd. Ayu 33 (3): 441-443. DOI: 10.4103/0974-8520.108863.

Wijayasiriwardene TDMCK, Herath HMIC, Premakumara GAS. 2016. Morphological and microscopic identification of *Curcuma albiflora* Thw. J Ayu Her Med 2 (1): 15-19. DOI: 10.31254/jahm.2016.2105.

Windarsih G, Utami DW, Yuriyah S. 2021. Morphological characteristics of Zingiberaceae in Serang District, Banten, Indonesia. Biodiversitas 22 (12): 5507-5529. DOI: 10.13057/biodiv/d221235.

Windarsih G, Riastiwi I, Dewi AP, Yuriyah S. 2022. Stomatal and epidermal characteristics of Zingiberaceae in Serang District, Banten, Indonesia. Biodiversitas 23: 5373-5386. DOI: 10.13057/biodiv/d231048.

Wu MH, Zhang W, Guo P, Zhao ZZ. 2014. Identification of seven Zingiberaceous species based on comparative anatomy of microscopic characteristics of seeds. Chin Med 9 (1): 1-7. DOI: 10.1186/1749-8546-9-10.

Xiao K, Mao X, Lin Y, Xu H, Zhu Y, Cai Q, Xie H, Zhang J. 2017. Trichome, a functional diversity phenotype in plant. Mol Biol 6 (1): 183. DOI: 10.4172/2168-9547.1000183.

Zahara M. 2020. Identification of morphological and stomatal characteristics of Zingiberaceae as medicinal plants in Banda Aceh, Indonesia. IOP Conf Ser Earth Environ Sci 425: 012046. DOI: 10.1088/1755-1315/425/1/012046.

Zhao ZZ, Hu YN, Wong YW, Wong WCG, Wu KIM, Jiang ZH, Kang T. 2005. Application of microscopy in authentication of Chinese patent medicine—Bo Ying compound. Microsc Res Technol 67 (6): 305-311. DOI: 10.1002/jemt.20213.

Zhao Z, Liang Z, Ping G. 2011. Macroscopic identification of Chinese medicinal materials: traditional experiences and modern understanding. J Ethnopharmacol 134 (3): 556-564. DOI: 10.1016/j.jep.2011.01.018.

Zhao H, Xiao MH, Zhong Y, Wang YQ. 2022. Leaf epidermal micromorphology of *Zingiber* (Zingiberaceae) from China and its systematic significance. PhytoKeys 190: 131-146. DOI: 10.3897/phytokeys.190.77526.